MULTI-GAUSSIAN ULTRASONIC BEAM MODELING

Lester W. Schmerr[+], Hak-Joon Kim[*], Ruiju Huang[#], and Alexander Sedov[##]
[+ * #]Center for Nondestructive Evaluation, Iowa State University, Ames, Iowa, USA
[##] Dept. of Mechanical Engineering, Lakehead University, Thunderbay, Ontario, Canada
lschmerr@cnde.iastate.edu

Abstract

A multi-Gaussian beam model is a computationally very efficient approach for modeling the sound beam generated by an ultrasonic piston transducer radiating into complex geometries and materials,. Here, we will demonstrate the remarkable versatility of multi-Gaussian beam modeling to solve for the propagation and transmission/reflection of focused and unfocused ultrasonic transducer beams through anisotropic media with curved interfaces. A new, highly modular approach will also be described that allows one to deal with very general modeling problems for piece-wise homogeneous multilayered media.

Introduction

Traditionally, the elastic waves generated by extended sources such as ultrasonic transducers have been modeled as a superposition of spherical waves or plane waves [1]. If, instead one uses Gaussian beams as basis functions for representing such sources, one obtains a highly efficient beam model that is also free from the singularities and caustics that occur with other functions [2],[3]. A multi-Gaussian beam model has the advantage over many other models in that the laws for propagation of the Gaussian beam and for its interaction with interfaces can be described in analytical terms so that it can easily handle interactions with multiple curved surfaces and complex media such as anisotropic solids. In this paper, we will discuss the propagation and transmission laws for Gaussian beams and show that these laws can be placed in a modular form that makes the solution expressions for even multi-layered anisotropic media very compact. Finally, since a multi-Gaussian beam model relies on the paraxial approximation, we will discuss the conditions under which that approximation may fail.

Propagation of a Gaussian Beam

The canonical problem that we will use to describe a multi-Gaussian beam model approach is shown in Fig. 1, where a single Gaussian beam radiates through a curved interface between a fluid and an anisotropic solid. In the fluid, the pressure at a distance, *D*, from its source can be expressed, for harmonic disturbances with time dependency of the form $\exp(-i\omega t)$ as

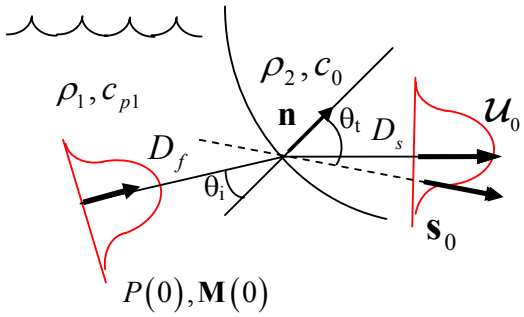

Figure 1: Transmission of a Gaussian beam through a fluid-anisotropic solid interface showing the propagation of the beam along the group velocity direction, $\mathcal{U}_0$. Snell's law relates the angles θ_i and θ_t, where θ_t is measured to the slowness vector, $\mathbf{s}_0$, in the solid from the unit normal, $\mathbf{n}$, to the interface.

$$p = P(D)\exp\left[i\omega\left(D/c_{p1} + \frac{1}{2}\mathbf{y}^T\mathbf{M}(D)\,\mathbf{y} - t\right)\right] \tag{1}$$

where c_{p1} is the wave speed in the fluid and *P(D)* and $\mathbf{M}(D)$ represent the "amplitude" and "phase" of the Gaussian beam, where **M** is a 2x2 symmetric matrix representing, in general, an elliptical cross section Gaussian beam. We place these terms in quotes since in actuality *P* and **M** are complex and hence both contain amplitude and phase components, but it is convenient to still refer to them in this manner. In the fluid if we seek a high frequency harmonic solution to the governing wave equation in the paraxial approximation of the type

$$p = A(y_1, y_2, D)\exp\left[i\omega\left(D/c_{p1} - t\right)\right] \tag{2}$$

we obtain the paraxial wave equation for *A* :

$$\frac{\partial^2 A}{\partial y_1^2} + \frac{\partial^2 A}{\partial y_2^2} + \frac{2i\omega}{c_{p1}}\frac{\partial A}{\partial D} = 0 \tag{3}$$

For the Gaussian beam of Eq. (1) A has the form

$$A = P(D)\exp\left[\frac{1}{2} i\omega \mathbf{y}^T \mathbf{M} \mathbf{y}\right] \tag{4}$$

Placing this expression into the paraxial wave equation, we obtain the governing equations for P and $\mathbf{M}$ as

$$\frac{dP}{dD} + \frac{c_{p1}}{2} P\, tr(\mathbf{M}) = 0 \tag{5a}$$

and

$$\frac{d\mathbf{M}}{dD} + c_{p1}\mathbf{M}\,\mathbf{M} = 0 \tag{5b}$$

The first of these equations is called the transport equation for the amplitude, P, and the second is a non-linear Ricatti equation for the phase, $\mathbf{M}$. It is, however, easy to solve for the phase since Eq. (5b) together with the relationship $\mathbf{M}\mathbf{M}^{-1} = \mathbf{I}$ allows one to obtain the linear equation

$$\frac{d\mathbf{M}^{-1}}{dD} = c_0 \mathbf{I} \tag{6}$$

the solution of which is

$$\mathbf{M}(D) = \mathbf{M}(0)\left[\mathbf{I} + c_{p1} D \mathbf{M}(0)\right]^{-1} \tag{7}$$

The transport equation can also be solved directly using the Ricatti equation and $\mathbf{M}\mathbf{M}^{-1} = \mathbf{I}$ again to yield

$$\frac{P(D)}{P(0)} = \sqrt{\frac{\det\left[\mathbf{M}(D)\right]}{\det\left[\mathbf{M}(0)\right]}} \tag{8}$$

Equations (7) and (8) are explicit relations for the propagation of the phase and amplitude, respectively, of the Gaussian beam in the fluid, and completely determine the Gaussian beam once the starting values $P(0), \mathbf{M}(0)$ are given.

In an anisotropic solid, the governing equations are more complex since we have [1]

$$C_{ijkl} \frac{\partial^2 u_k}{\partial x_j \partial x_l} = \rho_2 \frac{\partial^2 u_i}{\partial t^2} \tag{9}$$

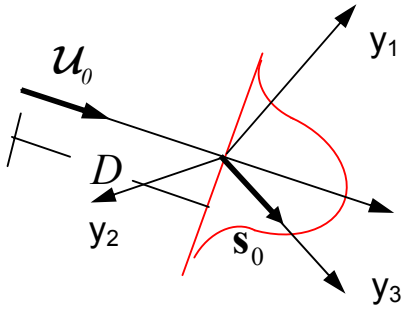

Figure 2: Propagation of a Gaussian beam through a distance D in an anisotropic solid along the group velocity direction but where a local set of slowness coordinates (y_1, y_2, y_3) are used to describe the Gaussian, where y_3 is in the direction of the slowness vector, $\mathbf{s}_0$.

where ρ_2 is the density of the solid, u_k are the displacements, and C_{ijkl} are the elastic constants. In spite of this complexity we can still obtain high frequency paraxial Gaussian beam solutions to these equations. The details are lengthy and cannot be given here but the general approach is outlined in [3]. One difference from the fluid case is we find the Gaussian beam solutions propagate along the group velocity direction, not the slowness direction, as shown in Fig. 1. Another difference, of course, is that the slowness itself is no longer a constant in the anisotropic solid. In fact we have three slowness surfaces that define the propagation of quasi-P waves and quasi-S1 and quasi-S2 shear waves [3] as a function of direction in the solid.

Although the Gaussian beam propagates along a group velocity direction, for the anisotropic case we have found that by expressing the propagating Gaussian in slowness rather than group velocity coordinates results in a significant reduction in the complexity of the resulting expressions. In slowness coordinates (y_1, y_2, y_3), where y_3 is along the slowness direction (see Fig. 2), the phase matrix is a symmetric 3x3 matrix, $\hat{\mathbf{M}}^{(y)}$. However, since in the group velocity coordinates the Gaussian phase matrix is only 2x2, as in the fluid case, one can show that all the 3-components of $\hat{\mathbf{M}}^{(y)}$ can be expressed in terms of the (y_1, y_2) components only (which define a symmetric 2x2 sub-matrix $\mathbf{M}^{(y)}$) since

$$\hat{M}_{I3}^{(y)} = -\frac{1}{c_0} M_{IJ}^{(y)} \mathcal{U}_{0J}^{(y)}$$
$$\hat{M}_{33}^{(y)} = \frac{1}{c_0} \hat{M}_{IJ}^{(y)} \mathcal{U}_{0I}^{(y)} \mathcal{U}_{0J}^{(y)} \qquad (I,J = 1,2 \; only) \qquad (10)$$

where c_0 is the wave speed for a particular wave type $0\left(0 = qP, qS1, qS2\right)$ and $\mathcal{U}_{0J}^{(y)}$ $\left(J = 1,2\right)$ are the components of the group velocity for the same particular wave type in the $\left(y_1, y_2\right)$ slowness coordinates. Thus, just as in the fluid case, the propagation of the Gaussian beam is completely determined once we obtain the 2x2 matrix $\mathbf{M}^{(y)}$ in slowness coordinates.

Here, we summarize the equations governing propagation of a Gaussian beam in an anisotropic solid. For a Gaussian beam, in slowness coordinates, we have

$$u_i\left(\mathbf{x}, \omega\right) = U\left(D\right) d_i \cdot \exp\left[i\omega \left(D / \mathcal{U}_0 + \frac{1}{2} \mathbf{y}^T \hat{\mathbf{M}}^{(y)}\left(D\right) \mathbf{y} - t \right) \right] \qquad (11)$$

where u_i are the displacement components, d_i are the polarization components and $\mathcal{U}_0$ is the magnitude of the group velocity for the given wave type. For this propagating beam we obtain the following equations:

$$\left(C_{ijkl} s_l s_j - \rho_2 \delta_{ik} \right) d_k = 0 \qquad (12)$$

$$\mathcal{U}_{0i} = \frac{C_{ijkl} s_l d_k d_j}{\rho_2} \qquad (13)$$

$$2\mathcal{U}_0 \frac{dU}{dD} + U \; tr\left(\mathbf{S}\, \mathbf{M}^{(y)} \right) = 0 \qquad (14)$$

and

$$\frac{d\mathbf{M}^{(y)}}{dD} + \frac{1}{\mathcal{U}_0} \mathbf{M}^{(y)}\, \mathbf{S}\, \mathbf{M}^{(y)} = 0 \qquad (15)$$

Equation (12) is Christoffel's equation which can be solved for the slowness and polarization. Equation (13) gives the corresponding group velocity from these slowness and polarization values. Equation (14) is the transport equation for the displacement amplitude, *U*, and Eq. (15) gives the Ricatti-like equation for the 2x2 matrix, $\mathbf{M}^{(y)}$. The 2x2 symmetric matrix, **S**, is also related to the properties of the slowness surface along the direction of propagation.

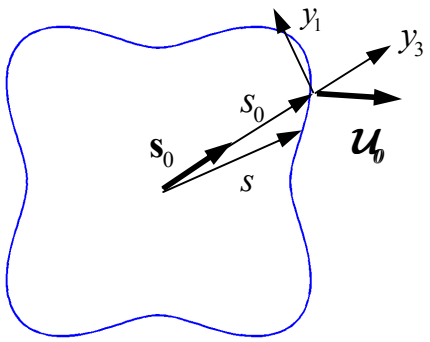

Figure 3: Cross section of a slowness surface for a quasi-shear wave in austenitic stainless steel showing the slowness vector, $\mathbf{s}_0$ for a particular direction, and the slowness, *s*, in the vicinity of this direction. The group velocity, $\mathcal{U}_0$, is normal to the slowness surface, as shown.

Figure 3 shows a cross-section of a particular slowness surface in the $\left(y_1, y_3\right)$ plane and the slowness *s* in the neighborhood of a given direction along which the slowness is s_0 and the group velocity is $\mathcal{U}_0$. Expanding the slowness, *s*, to second order in the $\left(y_1, y_2\right)$ slowness coordinates in the neighborhood of this given direction, we obtain [4]

$$s = s_0 + \hat{D}_J s_J + \hat{D}_{IJ} s_I s_J \qquad \left(I,J = 1,2\right) \qquad (16)$$

The components of the group velocity in the $\left(y_1, y_2\right)$ coordinates are given by $\mathcal{U}_{0J} = -c_0 \hat{D}_J$ and the **S** matrix components are just $S_{IJ} = -2c_0 \left(\hat{D}_{IJ} - \frac{1}{2s_0} \delta_{IJ} \right)$. Thus, we see that the **S** matrix is directly related to the curvatures $\hat{D}_{IJ}$ of the slowness surface in the given slowness direction. Although these curvatures cannot be obtained explicitly except for some simple anisotropic materials, they can be easily obtained numerically from the local properties of the slowness surface itself [4]. Equations (14) and (15) are very similar in form to the fluid case and, like that case, can be solved analytically. We obtain

$$\mathbf{M}^{(y)}(D)=\mathbf{M}^{(y)}(0)\left[\mathbf{I}+\frac{D}{\mathcal{U}_0}\mathbf{S}\mathbf{M}^{(y)}(0)\right]^{-1} \tag{17}$$

and

$$\frac{U(D)}{U(0)}=\frac{\sqrt{\det\left[\mathbf{M}^{(y)}(D)\right]}}{\sqrt{\det\left[\mathbf{M}^{(y)}(0)\right]}} \tag{18}$$

Equation pairs (7), (8) and (17), (18) describe the propagation of the Gaussian beam in the fluid and anisotropic solid, respectively, for the canonical problem in Fig. 1. To completely specify the solution for this problem, we now need to consider the laws that describe the transmission of the amplitude and phase of the Gaussian beam across the fluid-solid interface.

Transmission of a Gaussian beam across a curved interface

The transmission relation for the displacement amplitude of the Gaussian beam is particularly simple since the Gaussian beam is a high frequency solution whose amplitude is governed by the plane wave relation [3]

$$U(0)=T_{12}\left[\frac{P(D_f)}{-i\omega\rho_f c_{p1}}\right] \tag{19}$$

where T_{12} is just the plane wave transmission coefficient (based on displacement or velocity ratios) for a plane interface. Determining the transmission law for the phase is considerably more complex but straightforward. We match the phase of the incident and transmitted/ reflected waves to second order along the curved interface [3] to obtain

$$\begin{aligned}M^{(y)}_{PQ}(0)&=\left(G^A_{PI}\right)^{-1}\left(G^A_{QJ}\right)^{-1}G^f_{IK}G^f_{JM}M^{(y)}_{KM}(D_f)\\&+h_{IJ}\left(\frac{\cos\theta_i}{c_{p1}}-\frac{\cos\theta_t}{c_0}\right)\left(G^A_{PI}\right)^{-1}\left(G^A_{QJ}\right)^{-1}\end{aligned} \tag{20}$$

where

$$\mathbf{G}^A=\begin{bmatrix}\left(\cos\theta_i-\sin\theta_i\mathcal{U}_{01}/c_0\right) & -\sin\theta_i\,\mathcal{U}_{02}/c_0\\ 0 & 1\end{bmatrix},$$
$$\mathbf{G}^f=\begin{bmatrix}\cos\theta_i & 0\\ 0 & 1\end{bmatrix} \tag{21}$$

where h_{IJ} are the curvatures of the interface, as measured in plane of incidence coordinates and it is assumed, in Eq. (20) that the (y_1,y_3) is aligned with that plane. If that is not the case, then additional rotation matrices are needed in Eq. (20) [3].

A modular multi-Gaussian beam solution for multiple interfaces

Both the propagation and transmission laws we have described for the phase $\mathbf{M}^{(y)}$ relate this phase term when going from a point P_{j-1} to a point P_j, where these two points may be two separated points in the same material during propagation or two adjacent points at an interface relating the transmitted/reflected waves at an interface. In either case those laws can be written in the form

$$\mathbf{M}(P_j)=\left[\mathbf{D}\mathbf{M}(P_{j-1})+\mathbf{C}\right]\left[\mathbf{B}\mathbf{M}(P_{j-1})+\mathbf{A}\right]^{-1} \tag{22}$$

where **A**, **B**, **C**, **D** are 2x2 matrices. For example, for propagation through a distance D in the anisotropic solid we find

$$\mathbf{A}^{prop}=\begin{bmatrix}1 & 0\\ 0 & 1\end{bmatrix},$$
$$\mathbf{B}^{prop}=\frac{c_0 D}{\mathcal{U}_0}\begin{bmatrix}\left(c_0-2\hat{D}_{11}\right) & -2\hat{D}_{12}\\ -2\hat{D}_{12} & \left(c_0-2\hat{D}_{22}\right)\end{bmatrix},$$
$$\mathbf{C}_2^{prop}=\begin{bmatrix}0 & 0\\ 0 & 0\end{bmatrix},\ \mathbf{D}_2^{prop}=\begin{bmatrix}1 & 0\\ 0 & 1\end{bmatrix} \tag{23}$$

while for transmission across the fluid-solid interface

$$\mathbf{A}^{trans}=\begin{bmatrix}\dfrac{\cos\theta_t-\left(\mathcal{U}_{01}/c_0\right)\sin\theta_t}{\cos\theta_i} & 0\\ \dfrac{-\left(\mathcal{U}_{02}/c_0\right)\sin\theta_t}{\cos\theta_i} & 1\end{bmatrix},$$
$$\mathbf{B}^{trans}=\begin{bmatrix}0 & 0\\ 0 & 0\end{bmatrix},$$

$$\mathbf{C}^{trans} = \left(\frac{\cos\theta_i}{c_{p1}} - \frac{\cos\theta_t}{c_0} \right) \cdot \begin{bmatrix} \dfrac{h_{11} + h_{12}\left(\mathcal{U}_{02}/c_0\right)\sin\theta_t}{\left(\cos\theta_t - \left(\mathcal{U}_{01}/c_0\right)\sin\theta_t\right)\cos\theta_i} \\ \dfrac{h_{21}}{\cos\theta_i} \end{bmatrix} \begin{bmatrix} \dfrac{h_{12} + h_{22}\left(\mathcal{U}_{02}/c_0\right)\sin\theta_t}{\left(\cos\theta_t - \left(\mathcal{U}_{01}/c_0\right)\sin\theta_t\right)} \\ h_{22} \end{bmatrix}$$

$$\mathbf{D}^{trans} = \begin{bmatrix} \dfrac{\cos\theta_i}{\left(\cos\theta_t - \left(\mathcal{U}_{01}/c_0\right)\sin\theta_t\right)} & 0 \\ \dfrac{\left(\mathcal{U}_{02}/c_0\right)\sin\theta_t}{\left(\cos\theta_t - \left(\mathcal{U}_{01}/c_0\right)\sin\theta_t\right)} & 1 \end{bmatrix} \tag{24}$$

As a consequence of Eq. (22), when we have multiple propagation and transmissions/reflections occurring, such as in the weld problem of Fig. 4, we can show that we can directly relate the phase term in the final medium directly to its starting values through global matrices $\mathbf{A}^G, \mathbf{B}^G, \mathbf{C}^G, \mathbf{D}^G$, i.e.

$$\mathbf{M}\left(P_{M+1}\right) = \left[\mathbf{D}^G\mathbf{M}\left(P_0\right) + \mathbf{C}^G\right] \cdot \left[\mathbf{B}^G\mathbf{M}\left(P_0\right) + \mathbf{A}^G\right]^{-1} \tag{25}$$

where the global matrices are obtained simply through matrix products of all the modular propagation or transmission/reflection matrices along the given path, i.e.

$$\begin{bmatrix} \mathbf{A}^G & \mathbf{B}^G \\ \mathbf{C}^G & \mathbf{D}^G \end{bmatrix} = \begin{bmatrix} \mathbf{A}\left(P_{M+1}, P_M\right) & \mathbf{B}\left(P_{M+1}, P_M\right) \\ \mathbf{C}\left(P_{M+1}, P_M\right) & \mathbf{D}\left(P_{M+1}, P_M\right) \end{bmatrix} \cdot \begin{bmatrix} \mathbf{A}\left(P_M, P_{M-1}\right) & \mathbf{B}\left(P_M, P_{M-1}\right) \\ \mathbf{C}\left(P_M, P_{M-1}\right) & \mathbf{D}\left(P_M, P_{M-1}\right) \end{bmatrix} \cdots \cdot \begin{bmatrix} \mathbf{A}\left(P_1, P_0\right) & \mathbf{B}\left(P_1, P_0\right) \\ \mathbf{C}\left(P_1, P_0\right) & \mathbf{D}\left(P_1, P_0\right) \end{bmatrix} \tag{26}$$

This allows us to write the solution for the displacement wave field, even after M transmissions or reflections in the compact form

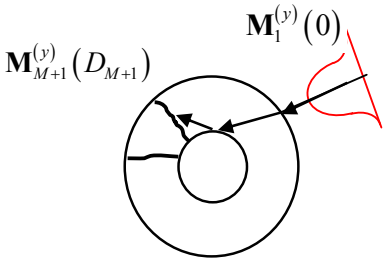

Figure 4: A Gaussian beam transmitted through a welded cylinder and reflected off the inner surface.

$$\mathbf{u}(\mathbf{x},\omega) = \frac{P(0)\mathbf{d}}{-i\omega\rho_1 c_{p1}} \prod_{m=1}^{M} T_{m\,m+1} \frac{\sqrt{\det\left[\mathbf{M}_{m+1}^{(y)}\left(D_{m+1}\right)\right]}}{\sqrt{\det\left[\mathbf{M}_{m+1}^{(y)}(0)\right]}} \cdot \frac{\sqrt{\det\left[\mathbf{M}_{m}^{(y)}\left(D_{m}\right)\right]}}{\sqrt{\det\left[\mathbf{M}_{m}^{(y)}(0)\right]}} \cdot \exp\left[i\omega\left(\sum_{m=1}^{M+1} D_m / \mathcal{U}_0^{(m)} - t \right)\right] \cdot \exp\left[i\omega\left(\frac{1}{2}\mathbf{y}^T\mathbf{M}_{M+1}^{(y)}\left(D_{M+1}\right)\mathbf{y} \right)\right] \tag{27}$$

where $\mathcal{U}_0^{(m)}$ is the magnitude of the group velocity along the wave path in the *m*th medium and $T_{m\,m+1}$ is a plane wave transmission or reflection coefficient when going from medium *m* to *m*+1. It is also possible to reduce the product of amplitude terms to a single term involving the global matrices [3]. However, we have found that in doing so one cannot calculate unambiguously the square roots of the resulting expressions, which are complex. The form of Eq. (27), however, results in explicit values for these terms.

A Multi-Gaussian beam model

Up to this point we have only considered a single Gaussian beam. However, Wen and Breazeale [5] have shown that by superposition of as few as ten Gaussians one can simulate the wave field of a circular, planar piston transducer and they gave the ten complex coefficients, A_n, B_n in their expansion. Thus, we need only take ten of our Gaussian beam solutions and relate their starting amplitude and phase terms, $\left[P(0)\right]_n, \left[\mathbf{M}(0)\right]_n$ $(n = 1, 2 \ldots 10)$ in the fluid to the A_n, B_n of Wen and Breazeale to obtain a solution for a planar piston source. We find

$$\begin{aligned}
&\left[P(0)\right]_n = \rho_1 c_{p1} v_0 A_n \\
&\left[M_{11}(0)\right]_n = \left[M_{22}(0)\right]_n = \frac{2iB_n}{\omega a^2} \\
&\left(M_{12} = M_{21} = 0\right)
\end{aligned} \tag{28}$$

where a is the radius of the transducer. Furthermore, we can also obtain the solution for a spherically focused piston transducer of focal length F by simply modifying the B_n coefficient as follows:

$$B_n \to \overline{B}_n = B_n + \frac{i\omega a^2}{2c_{p1}F} \tag{29}$$

Recently, Sha et. al. [6] also gave the solution for a rectangular planar piston transducer in terms of ten coefficients that are used along each axes of the source (for a total of 100 beams). In terms of their $\left(\hat{A}_n, \hat{B}_n\right)$ coefficients, we have

$$\begin{aligned}
&\left[P(0)\right]_{mn} = \rho_1 c_{p1} v_0 \hat{A}_n \hat{A}_m / \pi \\
&\left[M_{11}(0)\right]_{mn} = \frac{i}{\omega \hat{B}_n L_1^2}, \quad \left[M_{22}(0)\right]_{mn} = \frac{i}{\omega \hat{B}_m L_2^2} \\
&\left(M_{12} = M_{21} = 0\right)
\end{aligned} \tag{30}$$

One could also simulate a bi-cylindrically focused rectangular piston transducer with focal lengths $\left(F_1, F_2\right)$ from Sha's results by making the replacements

$$\hat{B}_n \to \frac{\hat{B}_n}{1 + i\omega \hat{B}_n / 2c_{p1}F_1}, \hat{B}_m \to \frac{\hat{B}_m}{1 + i\omega \hat{B}_m / 2c_{p1}F_2} \tag{31}$$

By combining these multi-Gaussian beam solution coefficients with the explicit propagation and transmission laws we have defined, one obtains a remarkably simple way to describe the behavior of the sound field from a number of different circular or rectangular piston probes for general multilayered, anisotropic media.

Limitations of the Paraxial approximation

The multi-Gaussian beam model is only an approximate solution since it rests fundamentally on the paraxial approximation, which can become inaccurate in some instances. For example, on transmission through an interface near a critical angle

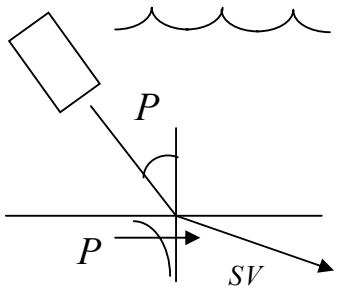

Figure 5: Transmission through a fluid-solid interface at the critical angle where the transmitted P-wave becomes an inhomogeneous wave along the interface.

as shown in Fig. 5, the transmission coefficient changes rapidly with small changes of angle. In the paraxial approximation it is assumed that this transmission coefficient is slowly varying, so that a paraxial solution may lose validity near such a critical angle.

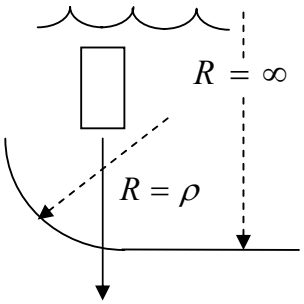

Figure 6: Transmission through an interface at a fillet where the surface curvature changes abruptly.

Similarly, Fig. 6 shows the case where the beam of a transducer is located in a region of the surface where the surface curvature suddenly changes. In this case, since different parts of the transmitted wave field encounter different curvatures, we cannot expect a multi-Gaussian beam model, which uses only a single curvature along the central transducer ray, to be valid.

As mentioned previously, multi-Gaussian solutions can also be used to model focused probes. However, if the probes are too tightly focused, as shown in Fig. 7, the waves from the transducer do not all travel approximately in the same direction, as assumed by the paraxial approximation. Many of the focused transducers used in NDE applications are not very tightly focused, so in that field the paraxial approximation may be perfectly adequate except for NDE applications involving, for example, acoustic microscopes.

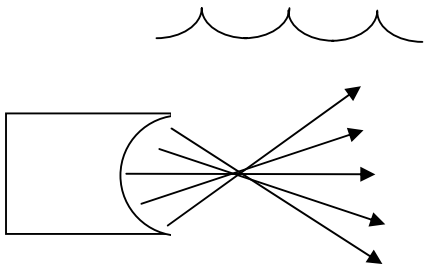

Figure 7: A tightly focused probe where the waves from the transducer do not all travel in approximately the same direction.

Finally, we mention the case shown in Fig. 8 where the transmitted beam at an interface is near grazing incidence. In this case the beam is highly distorted and other waves exist near the surface (surface waves, for example) that are not accounted for by the multi-Gaussian beam model, which only models the bulk-waves in the solid. Thus, in this case also we cannot expect our paraxial solutions to be accurate.

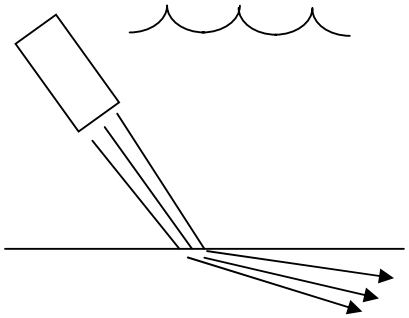

Figure 8: Transmission of a beam at an interface near grazing incidence.

Even though there are cases, as described here, where the paraxial multi-Gaussian beam model solutions may not be valid, there are also many practical situations where such situations do not occur and for which a multi-Gaussian beam model provides a powerful tool for accurately predicting the wave field of a transducer in very complex problems.

Summary and Conclusions

We have demonstrated that multi-Gaussian beam solutions can be explicitly constructed for complex problems where a piston probe interacts with multi-layered anisotropic materials. These solutions are computationally efficient and so can be used as the basis for parametric studies and real-time simulations. The only major limitation of these solutions is that they rely on paraxial approximations to the underlying governing equations. Thus, these solutions may lose accuracy in the cases described previously where the paraxial approximation is not valid. Work is on-going to define the limits of validity of the solutions presented here in those cases and to develop alternative beam models.

Acknowledgements

L. W. Schmerr, Hak-Joon Kim, and Ruiju Huang were supported in this work by the Center for NDE, Iowa State University through the National Science Foundation Industry/University Cooperative Research Center Program. A. Sedov would also like acknowledge the past support of the National Sciences and Engineering Research Council of Canada.

References

[1] L.W. Schmerr, Fundamentals of Ultrasonic Nondestructive Evaluation – A Modeling Approach, Plenum Press, New York, 1998.

[2] L.W. Schmerr, “A multi-Gaussian ultrasonic beam model for high performance simulations on a personal computer," Materials Evaluation, 58, 882-888, 2000.

[3] V. Cerveny, Seismic Ray Theory, Cambridge University Press, Cambridge, 2001.

[4] M. Rudolph, Ultrasonic Beam Models in Anisotropic Materials, PhD Thesis, Iowa State University, 1999.

[5] J.J. Wen and M.A. Breazeale,”A diffraction beam field expressed as the superposition of Gaussian beams, “ J. Acoust. Soc. Am., 83, 1752-1756, 1988.

[6] K. Sha, J. Yang, and W.S. Gan, “ A complex virtual source approach for calculating the diffraction beam field generated by a rectangular planar source,” IEEE Trans. on Ultrasonics, Ferroelectrics, and Frequency Control, 50, 890-896, 2003.

[7] L.W. Schmerr and A. Sedov, "A modular multi_Gaussian beam model for isotropic and anisotropic media," Review of Progress in Quantitative Nondestructive Evaluation, D.O. Thompson and D.E. Chimenti, Eds., American Institute of Physics, Melville, New York , 22A, 828-835, 2003.